Förster Transfer Outside the Weak-Excitation Limit

Brian A. Camley,[1] Frank L. H. Brown,[2,1,*] and Everett A. Lipman[1,†]

[1]*Department of Physics, University of California, Santa Barbara, California 93106, USA*
[2]*Department of Chemistry and Biochemistry, University of California, Santa Barbara, California 93106, USA*

The efficiency of resonance energy transfer can be used to determine nanometer-scale separations between dye molecules in a donor-acceptor pair. We argue that the standard method for making this determination in single-pair experiments is valid only when excitation by the applied field is much slower than the other photophysical processes in the system. We derive a simple relation between measured transfer efficiency and inter-dye distance that is valid regardless of excitation rate for a broad class of currently accepted models for dye photophysics. Significant deviations from weak-field results are predicted for typical experimental conditions.

PACS numbers: 82.20.Rp, 82.20.-w, 87.64.-t, 87.80.Nj

Förster Resonance Energy Transfer (FRET) is a near-field electromagnetic interaction that, owing to its strong distance dependence, has become a versatile tool for measuring nanometer-scale lengths in fields ranging from chemistry, materials science, and polymer science to biology and physics [1, 2]. Spectroscopic measurement [3] of FRET between fluorescent dyes is widely used in molecular biophysics to determine structures and dynamics of proteins, DNA, RNA, and supramolecular assemblies (protein oligomers, membranes, etc.) [1, 2, 4]. Techniques [5] for measuring FRET from a single directly-excited donor dye (D) to a single acceptor (A) have revealed biomolecular behavior previously cloaked by ensemble averaging [4, 6–11].

Distance measurements using FRET commonly rely on the implicit assumption that the rate of donor excitation is small compared with other photophysical rates in the system. Although this assumption is clearly valid for early experiments demonstrating the utility of FRET as a "spectroscopic ruler" [3], modern single-pair FRET (spRET) measurements often require rapid excitation for useful time resolution and signal quality. Under conditions encountered in many spRET experiments, the validity of the weak-field assumption is questionable. Here we derive a relation between donor-acceptor separation and the efficiency of energy transfer (see below) measured in typical spRET experiments. This relation emerges from a broad class of currently-accepted photophysical models, and is valid regardless of excitation rate. Significant deviations of our relation from its weak-field counterpart may help to explain unexpected results in spRET control experiments [6, 12–14].

Using a dipole approximation, Förster [15] calculated the rate constant for energy transfer between the donor-excited (D^*A) and acceptor-excited (DA^*) states of a dye pair:

$$k_T = \frac{1}{\tau_D}\left(\frac{R_0}{R}\right)^6, \tag{1}$$

where τ_D is the donor fluorescence lifetime observed in the absence of an acceptor, R is the separation of the dyes, and R_0 is the Förster radius, at which 50% of donor excitations relax from D^*A via transfer. R_0 can be determined by spectroscopic measurements that do not involve FRET [1]. The "efficiency of energy transfer" E [2] is the probability that a single donor excitation will be transferred from D^*A to DA^*:

$$E \equiv \frac{k_T}{k_T + \tau_D^{-1}} = \frac{1}{1 + (R/R_0)^6}. \tag{2}$$

The "measured transfer efficiency" $\mathcal{E}$ obtained by photon counting is related to E, but in general they are not equivalent. In ratiometric spRET experiments [6],

$$\mathcal{E} \equiv \frac{N_A}{N_A + \gamma N_D} = \frac{\rho_A}{\rho_A + (\phi_A/\phi_D)\rho_D}, \tag{3}$$

where for donor or acceptor, N is the number of photons detected, ρ is the rate of photon emission, and ϕ is the fluorescence quantum yield in the absence of the other dye (e.g., $\phi_D = k_D\tau_D$, where k_D is the rate constant for donor fluorescence). The correction factor $\gamma = \eta_A\phi_A/\eta_D\phi_D$, where η is the detection efficiency for fluorescence emitted by the indicated dye. For sufficiently long measurements, number fluctuations will be small, and the second equality follows. We do not consider detector dead times, position-dependent detection efficiencies, and other experimental effects assumed to be small under typical conditions. As we show below, γ has been chosen so that when excitation of the donor is much slower than all other rates in the problem, $\mathcal{E} \to E$. However, if the excitation rate is not small, a full kinetic analysis can lead to differences between E and $\mathcal{E}$, even for relatively simple kinetic models such as that shown in Fig. 1 [16–18].

In what follows, we show that for a broad class of kinetic models of dye photophysics,

$$\mathcal{E} = \frac{1}{\Lambda + (R/R_0)^6}. \tag{4}$$

Λ can depend on all rates in the problem other than k_T; it is independent of R. We calculate $\mathcal{E}$ for two physically relevant models, and show that for typical spRET parameters, Λ can be significantly larger than its weak-field value of 1. The measured transfer efficiency will then be less than unity even at distances much smaller than R_0. Physically, $\Lambda > 1$ reflects the inability of doubly-excited dye pairs to undergo FRET within commonly accepted photophysical models.

*Electronic address: flbrown@chem.ucsb.edu
†Electronic address: lipman@physics.ucsb.edu

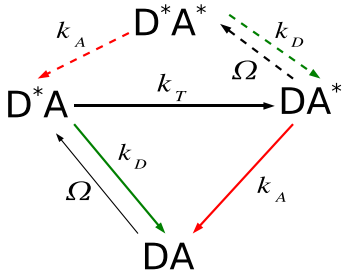

FIG. 1: Minimal FRET kinetic diagram. At low field strengths ($\Omega \ll k_T, k_D, k_A$), the dashed transitions may be ignored, and $\mathcal{E} = E$. Equations 4 and 7 are valid for the complete model. The rate matrix for this scheme, shown in Eq. 6, corresponds to a state probability vector $\mathbf{P}^\dagger = (P_{D^*A}, P_{DA^*}, P_{DA}, P_{D^*A^*})$. The rate constants Ω, k_T, k_D, and k_A are for field-induced excitation of the donor, Förster transfer (Eq. 1), and photon emission by the donor and acceptor, respectively.

To evaluate Eq. 3 within any FRET kinetic model, we express ρ_A and ρ_D in terms of the steady-state occupation probabilities of the states from which fluorescence originates and the associated rate constants. For example, the kinetic scheme shown in Fig. 1 implies that $\rho_A = k_A(P^{ss}_{DA^*} + P^{ss}_{D^*A^*})$. Steady state probabilities are calculated from the stationary solution of the master equation $\dot{\mathbf{P}}(t) = \mathbb{W}\mathbf{P}(t)$ [19] associated with the kinetic model, so that

$$\mathbb{W}\mathbf{P}^{ss} = \begin{pmatrix} W_{11} & W_{12} & \cdots & W_{1N} \\ W_{21} & W_{22} & \cdots & W_{2N} \\ \vdots & \vdots & \ddots & \vdots \\ W_{N1} & W_{N2} & \cdots & W_{NN} \end{pmatrix} \begin{pmatrix} P^{ss}_{D^*A} \\ P^{ss}_{DA^*} \\ \vdots \\ P^{ss}_{N} \end{pmatrix} = 0. \qquad (5)$$

Here, and in all that follows, we order the kinetic states so that the first two components of $\mathbf{P}$ are $P^{ss}_{D^*A}$ and $P^{ss}_{DA^*}$.

As a simple example, the four state model of Fig. 1 has the rate matrix

$$\mathbb{W}_4 = \begin{pmatrix} -(k_T + k_D) & 0 & \Omega & k_A \\ k_T & -(k_A + \Omega) & 0 & k_D \\ k_D & k_A & -\Omega & 0 \\ 0 & \Omega & 0 & -(k_A + k_D) \end{pmatrix}. \qquad (6)$$

It is straightforward to solve Eq. 5 for the steady-state probabilities [16], which give us the measured efficiency $\mathcal{E}$ through Eq. 3. For $\mathbb{W} = \mathbb{W}_4$, $\mathcal{E}$ takes the form of Eq. 4, with

$$\Lambda_4 = 1 + \frac{\Omega k_D}{k_A(\Omega + k_A + k_D)}. \qquad (7)$$

Our main point is that Eq. 4 applies much more broadly than this specific case. In fact, Eq. 4 will result from any probability-conserving kinetic model obeying the following three properties:

1. The kinetic scheme associated with $\mathbb{W}$ is "ergodic" [19] in the sense that it is possible to connect any two states by following arrows in the diagram.

2. The only effect of inter-dye interaction is that $\mathbb{W}$ couples two states via Förster transfer ($D^*A \rightarrow DA^*$). Given our ordering convention for $\mathbf{P}$, this means that only elements W_{11} and W_{21} of $\mathbb{W}$ contain k_T, and, by extension, only these two elements contain any dependence on inter-dye separation.

3. Förster transfer is the only mechanism by which A can become excited, i.e., direct excitation of A is negligible.

If $\mathbb{W}$ is a well-defined rate matrix, property 1 is sufficient to guarantee that a unique normalized $\mathbf{P}^{ss}$ exists, and that all elements of this vector are non-zero [19].

Because $\sum_{i=1}^{N} W_{ij} = 0$ for any rate matrix that conserves probability [19], each row of (5) is linearly dependent on all the others. We are therefore free to eliminate the first equation, corresponding to the topmost row. Taking advantage of the fact that the ratio of rates appearing in Eq. 3 is not sensitive to the normalization of $\mathbf{P}^{ss}$, we set $P^{ss}_{D^*A} = 1$. The equations for the remaining $N-1$ unnormalized steady-state "probabilities" then become

$$\begin{pmatrix} W_{22} & \cdots & W_{2N} \\ \vdots & \ddots & \vdots \\ W_{N2} & \cdots & W_{NN} \end{pmatrix} \begin{pmatrix} P^{ss}_{DA^*} \\ \vdots \\ P^{ss}_{N} \end{pmatrix} = \begin{pmatrix} -W_{21} \\ \vdots \\ -W_{N1} \end{pmatrix}. \qquad (8)$$

This equation can be inverted, and since k_T appears only in linear order on the right-hand side of Eq. 8, and nowhere on the left (see property 2), each element of $\mathbf{P}^{ss}$ must take the form $u + v\,k_T$, where u and v are independent of k_T. Using Eq. 3, we conclude that $\mathcal{E} = (a + b\,k_T)/(c + d\,k_T)$, where a, b, c, and d can depend on any of the rate constants in the FRET kinetic scheme except for k_T. Property 3 tells us that $\rho_A \rightarrow 0$ as $k_T \rightarrow 0$, and it follows that $\mathcal{E}$ must also approach zero as $k_T \rightarrow 0$. We conclude that $a = 0$. Using Eq. 1, we obtain $\mathcal{E}^{-1} = \Lambda + \beta(R/R_0)^6$. Both $\Lambda \equiv d/b$ and $\beta \equiv c\tau_D/b$ are independent of R.

The value assumed by β can be found by considering Eq. 3 in the limit where k_T is by far the smallest rate constant in the problem (i.e., $R \gg R_0$). In this limit, the expressions for the photon emission rates reduce to $\rho_D = k_D P^{ss}_{D^*A}$ and $\rho_A = k_T \phi_A P^{ss}_{D^*A}$ [20]. Equation 3 gives $\mathcal{E} \rightarrow \left(\frac{R_0}{R}\right)^6$ in the large R limit. The expression from the preceding paragraph predicts $\mathcal{E} \rightarrow \beta^{-1}\left(\frac{R_0}{R}\right)^6$ in the same limit, and thus $\beta = 1$.

In the limit where Ω is by far the smallest rate constant in the problem, the photon emission rates reduce to $\rho_D = \Omega k_D/(k_T + \tau_D^{-1})$ and $\rho_A = \Omega\phi_A k_T/(k_T + \tau_D^{-1})$ [21]. Use of these expressions in Eq. 3 yields $\mathcal{E} = E$, justifying the assertion that the normally assumed expression for $\mathcal{E}$ is, in fact, a weak-field result.

A notable consequence of this analysis is that $\mathcal{E}$ is not expected to approach one as $R \rightarrow 0$. Instead, $\mathcal{E} \rightarrow \Lambda^{-1}$ as $R \rightarrow 0$ ($\Lambda \geq 1$ by Eq. 3). The $\mathcal{E}(R/R_0)$ curve will also be less steep near $R = R_0$, with a slope $-6/(1+\Lambda)^2$ rather than the usual $-3/2$ obtained when $\Lambda = 1$.

Analytical expressions for Λ are, in principle, obtainable for arbitrarily complex kinetic schemes, as Eq. 8 can always be solved by elementary row operations. In practice, the expressions become unwieldy for moderately complex models, and it is helpful to employ symbolic manipulation software

and/or numerical methods. We treat one special case of physical interest—a nine-state scheme, incorporating triplet states and intersystem crossing for both dyes (Fig. 2). This model

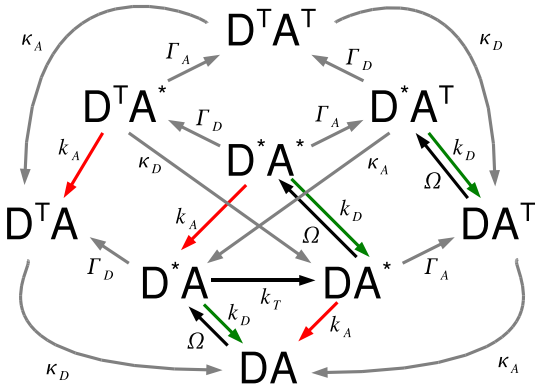

FIG. 2: Kinetic scheme for a nine-state model including donor and acceptor triplet states. Here $\rho_A = k_A(P^{ss}_{DA^*} + P^{ss}_{D^TA^*} + P^{ss}_{D^*A^*})$, and $\rho_D = k_D(P^{ss}_{D^*A} + P^{ss}_{D^*A^T} + P^{ss}_{D^*A^*})$. Rate constants not appearing in Fig. 1 are for intersystem crossing to (Γ_D, Γ_A) and from (κ_D, κ_A) the triplet states.

is commonly used to describe fluorescent dye excitation and blinking [17, 22]. Λ_9 is exceedingly complex; we do not present the analytical expression here. For a rough numerical estimate, we can use photophysical parameters for rhodamine 6G in water [22] ($k_D = k_A = 250\ \mu s^{-1}$, $\Gamma_D = \Gamma_A = 1\ \mu s^{-1}$, and $\kappa_D = \kappa_A = 0.5\ \mu s^{-1}$) and $\Omega_0 \approx 40\ \mu s^{-1}$ (the peak excitation rate in Ref. 13), giving us $\Lambda_9 = 1.32$ or $\mathcal{E}_{\max} = 0.76$. This suggests that the effects predicted by Eq. 4 should be experimentally observable (see below for a more detailed comparison with experiment). More generally, Fig. 3 is a plot of $\mathcal{E}$ from the nine-state model as a function of R/R_0 for a series of different excitation rates Ω. The curves exhibit significant differences between $\mathcal{E}$ and E, and it would appear that if the nine-state model is applicable, Eq. 4 will be essential for interpreting experiments wherein Ω exceeds a few percent of k_D.

Physically, we can interpret $\mathcal{E} < 1$ at small distances as a "jamming" phenomenon. At high Ω, it becomes likely that the donor and acceptor will be simultaneously excited (D^*A^* or D^*A^T), precluding normal Förster transfer. Depending on the details of the kinetic diagram, it may be the case that the donor is likely to cycle between D and D^* multiple times before the acceptor returns to the ground state. As a consequence, $\mathcal{E}$ will be reduced relative to the weak-field result (Eq. 2). This discussion clarifies our definition of "weak": $\mathcal{E} = E$ if Ω is much smaller than all other rate constants in the kinetic scheme. The naive condition $\Omega \ll k_D, k_A$ does not guarantee that $\mathcal{E} = E$ for our nine-state scheme, since jamming by A^T may lower $\mathcal{E}$ if Ω is comparable to κ_A. This picture allows for a qualitative description of Λ_9 as a function of rate constants. Increasing Ω, increasing the intersystem crossing rate Γ_A, and decreasing the triplet decay rate κ_A all increase the amount of time spent in a doubly-excited state where donor cycling is possible, and thus increase Λ_9.

The analysis presented above is formally restricted to

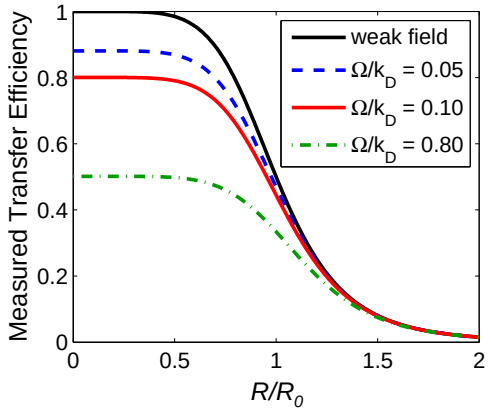

FIG. 3: Measured transfer efficiency $\mathcal{E}$ (Eq. 4) as a function of dye separation for the nine-state system of Fig. 2. Multiple excitation rates are considered, and we use typical photophysical parameters [22] $k_D = k_A = 250\ \mu s^{-1}$, $\Gamma_D = \Gamma_A = 2.5\ \mu s^{-1}$, $\kappa_D = \kappa_A = 1.0\ \mu s^{-1}$, and detection efficiencies $\eta_A = \eta_D$. In the "weak-field" case, $\mathcal{E} = E$ (Eq. 2).

continuous-wave (CW) excitation sources (we assume Ω is constant in time), and the limit of long measurement times (see Eq. 3 and subsequent discussion). We do not consider the question of fluctuations in finite-duration measurements, but do note that excitation strength will affect the full spRET efficiency distributions, particularly when the sample is diffusing through the exciting beam (see next section). Pulsed excitation sources do not alter the physical picture discussed in the preceding paragraph. The time-independent kinetic formulation appropriate to CW experiments is easily extended to the case where excitation occurs impulsively at periodically spaced time points. Evolution of the probability vector then involves two matrices, a zero-field rate matrix $\mathbb{W}_{\Omega=0}$ governing dynamics for all times between exciting pulses, and a pulse-effect matrix that acts to instantaneously excite all $D \to D^*$ transitions with probability P_e. At long times, the system settles into a periodic steady-state that can be calculated numerically. The associated periodic probability vector may be used to calculate a measured transfer efficiency for pulsed excitation, $\mathcal{E}_p$, averaged over many pulse cycles. Although our simple functional form for $\mathcal{E}$ (Eq. 4) does not strictly hold for $\mathcal{E}_p$, the two curves are similar so long as care is taken to compare experiments that share the same average rate of excitation. That is, for a pulse repetition rate $f_{\rm rep}$, $\Omega_p \equiv P_e f_{\rm rep}$ must correspond to the CW Ω discussed elsewhere in this work.

The differences that do arise between pulsed and CW excitation depend upon the complex interplay of all rate constants in the problem, including $f_{\rm rep}$; depending on Ω, $f_{\rm rep}$, and dye photophysics, it is possible to find situations where $\mathcal{E}_p > \mathcal{E}$, $\mathcal{E}_p < \mathcal{E}$, and even cases in which the relative behavior changes depending upon inter-dye separation. In the limit of $P_e \to 0$ and $f_{\rm rep} \to \infty$ with Ω_p held constant, $\mathcal{E}_p$ approaches the CW result $\mathcal{E}$ calculated with $\Omega = \Omega_p$. For the 9-state model and physical parameters discussed above, the two curves $\mathcal{E}$ and $\mathcal{E}_p$ are nearly indistinguishable for values of $P_e < 0.1$ ($f_{\rm rep}$ greater

than a few hundred MHz).

In a commonly-used experimental configuration[23], a 40 MHz picosecond pulsed laser with average power in the tens to low hundreds of microwatts is used for excitation. Although details of the optical path introduce considerable uncertainty in P_e (see next section), at the center of a diffraction-limited focus $P_e \approx 0.9$ for this source (60 μW) and a typical donor dye. Consequently, $\Omega_p \approx 35\ \mu s^{-1}$, and measurable jamming effects would be expected within the 9-state model.

Comparison with experiment

The preferred experimental test of Eq. 4 would involve measurements on completely immobilized dye pairs fixed at constant separation, relative orientation, and position within the exciting beam. The photophysics of both dyes would be fully characterized, and the irradiance of the beam at the donor dye location would be precisely controllable. Experiments performed to date deviate substantially from this idealized scenario. Dyes commonly used for spRET are not fully characterized, flexible molecular linkers cause inter-dye separation and relative orientation to vary with time, and most high-irradiance experiments are carried out with freely diffusing samples (i.e., the dye-pair complex is undergoing 3-D Brownian motion in and out of the laser focus).

If a donor molecule with absorption cross-section [24] σ is exposed to a beam of irradiance (power per unit area) I, the excitation rate

$$\Omega = \frac{I}{h\nu}\sigma, \tag{9}$$

where h is Planck's constant and ν is the frequency of the laser. Because the extreme sensitivity of high numerical aperture optics to aberrations hinders estimation of I, it is difficult to determine Ω for a given experiment. Seemingly insignificant details, for example a 10% coverslip thickness variation or a difference of a few microns in focal position, can change the peak irradiance by a factor of two [25].

A rough estimate of the excitation rate at the center of focus in Ref. 13 is $\Omega_0 \approx 40\ \mu s^{-1}$, about 20% of the fluorescence rate $1/k_D$ of the donor. Figure 3 shows that the measured FRET efficiency at $\Omega/k_D \approx 20\%$ ($\Lambda_9 \approx 1.3$) would be significantly different than the result predicted by the weak field theory. The vast majority of molecules in a non-tethered, solution-phase single-molecule experiment do not, however, see the peak intensity while diffusing through the beam focus, so we expect an effective Λ closer to one. In Ref. 13, the average measured efficiency never exceeds 0.95, even though the dyes are believed to come within $0.35R_0$ of each other; $E(R = 0.35R_0) = 0.998$. Other experiments show similar deviations [6, 7, 9, 12, 14]. It should be noted that the microscope objective used in Ref. 13 was not designed to make measurements in solution, and experiments using the same laser input power with a well-adjusted modern water-immersion objective could easily have peak values of Ω four times higher.

To enable quantitative comparison with existing experiments, we supplement the kinetic picture of Fig. 2 to include rotational diffusion of the two dyes and translational diffusion of the dye pair. Translation of the pair makes Ω time dependent [$\Omega(r(t)) = \Omega_0 e^{-2r(t)^2/w^2}$] as the pair's distance from an isotropic 3-D Gaussian beam focus at $r = 0$ (with $1/e^2$ radius w) fluctuates in time. Rotation of the two dyes adds time dependence to k_T [$k_T(\kappa^2(t)) = \frac{3\kappa^2(t)}{2\tau_D}\left(\frac{R_0}{R}\right)^6$] as the relative orientation of the two dyes evolves in time, affecting the value of the "κ^2 factor" [2]. Translational and rotational diffusion are assumed isotropic and independent, with diffusion constants D_T and D_R, respectively.

To calculate $\mathcal{E}$ within this extended model, we generate stochastic trajectories for $r(t)$ and $\kappa^2(t)$ via Brownian dynamics simulations for the radial position of the pair and orientation of the two dyes. N_A and N_D for a given trajectory are determined by kinetic Monte Carlo simulations [26] applied to the kinetic scheme of Fig. 2 generalized to include $\Omega(r(t))$ and $k_T(\kappa^2(t))$. Averaging over both kinetic and stochastic trajectories yields numerical predictions for $\mathcal{E}$. It was observed in preliminary calculations that translational diffusion is sufficiently slow to justify use of a limiting behavior discussed previously [17, 18]. This allows us to calculate $\rho_A = \int \tilde{\rho}_A(\Omega(r))d^3r$ with $\tilde{\rho}_A(\Omega) = \frac{d}{dt}\langle N_A(\Omega)\rangle_{\text{rot,MC}}$ (similarly for ρ_D), i.e., $\tilde{\rho}_{A(D)}(\Omega)$ is the average rate of acceptor (donor) emission assuming the pair is fixed at position r, but dye rotation and kinetics are fully sampled numerically. The integral is evaluated by quadrature.

We have used the above procedure to compare with the experiments reported in Ref. 13. In that work, the following physical parameters are known: $D_T \approx 1\ \mu m^2/ms$, $D_R \approx 0.6\ ns^{-1}$, $w \approx 200$ nm, $\Omega_0 \approx 40\ \mu s^{-1}$, $k_A \approx k_D \approx 250\ \mu s^{-1}$. The remaining photophysical rate constants for the specific dye pair used are not precisely characterized. Representative generic estimates often quoted by the community include [22]: $\Gamma_D \approx \Gamma_A \approx 1\ \mu s^{-1}$ and $\kappa_D \approx \kappa_A \approx 1\ \mu s^{-1}$. We find that tuning these numbers by a factor of two leads to a favorable comparison with the experimental data (Fig. 4). It should stressed that a naive best fit of Eq. 4 to the experimental data does a far superior job than the standard result of Eq. 2. The addition of translational and rotational motion violates assumption 2 in our derivation and renders Eq. 4 inexact, but the proposed functional form remains a good approximation suitable for describing experimental data.

Though we have considered a specific kinetic model in detail, Eq. 4 applies to a broad class of photophysical models of immobilized dyes. The most restrictive of our assumptions is the unique donor-acceptor transfer pathway [28]. Because of this, our form for $\mathcal{E}$, like the traditional weak-field limit, does not apply directly to schemes with conformational, translational or orientational dynamics of the two dyes (e.g., Fig. 1c of Ref. 17). However, our result is readily extended to the usual fast and slow modulation limits [13, 29]. Furthermore, we have demonstrated our expression for $\mathcal{E}$ remains a good approximation in the presence of pair translation and rotational motion of the dyes for typical experimental conditions.

Equation 4 is expected to produce correct predictions for immobilized dye pairs, subject to the underlying assumptions of our kinetic models for dye photophysics. We stress that these assumptions, although consistent with literature prece-

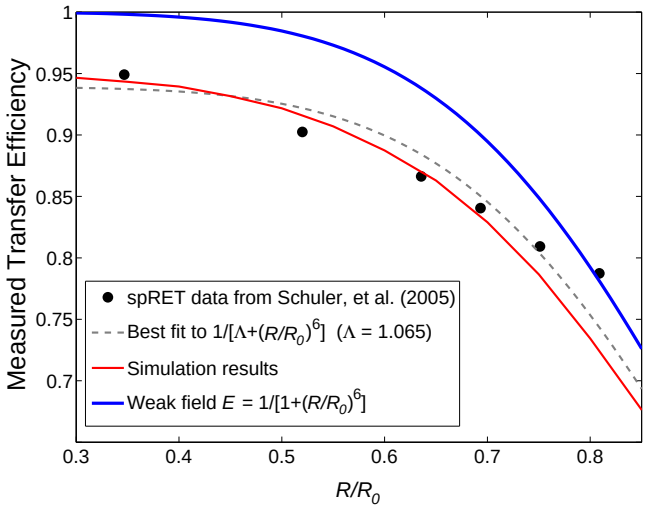

FIG. 4: Measured transfer efficiency $\mathcal{E}$ (Eq. 3) for the nine-state system of Fig. 2 in the slow-diffusion limit. Parameters selected for the simulations were $\Gamma_D = \Gamma_A = 1.25\ \mu s^{-1}$, $\kappa_D = \kappa_A = 2\ \mu s^{-1}$, and $\eta_A = \eta_D$. Black dots are experimental spRET data from Ref. 13 for separations $R < R_0$; the larger separations measured in that work are severely affected by kinks in the polyproline oligomers separating the dyes [10, 27], and are not considered.

dent [17, 22, 30], have not been verified experimentally. The dyes commonly used in single-pair FRET experiments are not yet well-characterized, and it is possible, perhaps even likely, that the true photophysics of spRET pairs cannot be accounted for within the confines of our assumptions. For example, we implicitly assume the absence of multiple excitation "annihilation" that is observed to be an important process for certain multichromophoric dendrimers [31, 32]. One can imagine many other photophysical processes that would involve additional separation-dependent interactions and/or transfer pathways between two dyes. Any such complications could limit the applicability of our expression for $\mathcal{E}$.

Equation 4 is an inescapable consequence of the models presently used to analyze spRET. Either these models are valid, in which case Eq. 4 must be employed to accurately interpret experiments, or new theory is needed that better describes the behavior of real fluorophores. Further examination of the photophysics of these systems will clearly be necessary before the full potential of spRET measurements can be realized. We therefore hope that this work will serve to motivate detailed characterization of commonly-used dye pairs.

Acknowledgments

We thank William Eaton, Henrik Flyvbjerg, Irina Gopich, Dmitrii Makarov, Don Marolf, Amit Meller, Ben Schuler, Attila Szabo, and Haw Yang for helpful discussions. B.A.C. acknowledges the support of the Fannie and John Hertz Foundation. F.L.H.B. and E.A.L are Alfred P. Sloan research fellows. F.L.H.B. is a Camille Dreyfus Teacher-Scholar. This work was supported in part by the National Science Foundation (grant no. CHE-0848809).

[1] B. W. VanDerMeer, G. Coker, and S. Y. S. Chen, *Resonance Energy Transfer: Theory and Data* (Wiley, 1994).
[2] R. M. Clegg, in *Fluorescence Imaging Spectroscopy and Microscopy*, edited by X. F. Wang and B. Herman (Wiley-Interscience, 1996), chap. 7, pp. 179–252.
[3] L. Stryer and R. P. Haugland, Proc. Natl. Acad. Sci. U. S. A. **58**, 719 (1967).
[4] S. Weiss, Science **283**, 1676 (1999).
[5] T. Ha, T. Enderle, D. F. Ogletree, D. S. Chemla, P. R. Selvin, and S. Weiss, Proc. Natl. Acad. Sci. U. S. A. **93**, 6264 (1996).
[6] A. A. Deniz, M. Dahan, J. R. Grunwell, T. J. Ha, A. E. Faulhaber, D. S. Chemla, S. Weiss, and P. G. Schultz, Proc. Natl. Acad. Sci. U. S. A. **96**, 3670 (1999).
[7] B. Schuler, E. A. Lipman, and W. A. Eaton, Nature **419**, 743 (2002).
[8] E. A. Lipman, B. Schuler, O. Bakajin, and W. A. Eaton, Science **301**, 1233 (2003).
[9] H. W. Liu, G. Cosa, C. F. Landes, Y. N. Zeng, B. J. Kovaleski, D. G. Mullen, G. Barany, K. Musier-Forsyth, and P. F. Barbara, Biophys. J. **89**, 3470 (2005).
[10] L. P. Watkins, H. Y. Chang, and H. Yang, J. Phys. Chem. A **110**, 5191 (2006).
[11] C. Gell, D. Brockwell, and A. Smith, *Handbook of Single Molecule Fluorescence Spectroscopy* (Oxford University Press, Oxford, 2006).
[12] N. K. Lee, A. N. Kapanidis, Y. Wang, X. Michalet, J. Mukhopadhyay, R. H. Ebright, and S. Weiss, Biophys. J. **88**, 2939 (2005).
[13] B. Schuler, E. A. Lipman, P. J. Steinbach, M. Kumke, and W. A. Eaton, Proc. Natl. Acad. Sci. U. S. A. **102**, 2754 (2005).
[14] H. Sahoo, D. Roccatano, A. Hennig, and W. M. Nau, J. Am. Chem. Soc. **129**, 9762 (2007).
[15] T. Förster, Annalen Der Physik **2**, 55 (1948).
[16] Z. S. Wang and D. E. Makarov, J. Phys. Chem. B **107**, 5617 (2003).
[17] I. Gopich and A. Szabo, J. Chem. Phys. **122**, 014707 (2005).
[18] I. V. Gopich and A. Szabo, J. Phys. Chem. B **111**, 12925 (2007).
[19] R. Zwanzig, *Nonequilibrium Statistical Mechanics* (Oxford University Press, USA, 2001).
[20] Donor emission is dominated by D^*A, since A is seldom excited in this limit. The rate limiting step for acceptor emission is the $D^*A \rightarrow DA^*$ transition. The factor of ϕ_A transforms the rate for occurrence of this transition into the rate of acceptor fluorescence by counting only the fraction of A^* excitations that eventually fluoresce. This simple correction requires that the intramolecular rate constants of the acceptor do not depend on the donor's state, a condition mandated by property 2 above.
[21] The rate-limiting step for emission by either D or A is the excitation transition, which occurs with rate Ω (The system is almost always in the DA ground state because of the weak excitation conditions). The factors multiplying Ω in the emission rates reflect the probabilities that a single excitation beginning in D^*A ultimately yields either a donor or acceptor photon.
[22] J. Widengren, U. Mets, and R. Rigler, J. Phys. Chem. **99**, 13368

(1995).
[23] X. X. Kong, E. Nir, K. Hamadani, and S. Weiss, J. Am. Chem. Soc. **129**, 4643 (2007).
[24] A typical donor cross section is 2.8×10^{-20} m^2 (Alexa Fluor 488 at 493 nm).
[25] H. E. Keller, in *Handbook of Biological Confocal Microscopy*, edited by J. B. Pawley (Springer, 1995), chap. 7, pp. 111–126, 2nd ed.
[26] D. T. Gillespie, J. Phys. Chem. **81**, 2340 (1977).
[27] R. B. Best, K. A. Merchant, I. V. Gopich, B. Schuler, A. Bax, and W. A. Eaton, Proc. Natl. Acad. Sci. U. S. A. **104**, 18964 (2007).
[28] We stress that the starting point for this work is Eq. 1 for k_T. Competing transfer mechanisms, breakdown of the dipole approximation, and/or technical details related to photon detection may also lead to deviations between experimentally measured transfer efficiencies and our theory. Acceptor photobleaching [23] can also reduce $\mathcal{E}$ if data from donor-only sample molecules is not eliminated.
[29] R. E. Dale, J. Eisinger, and W. E. Blumberg, Biophys. J. **26**, 161 (1979).
[30] D. Nettels, I. V. Gopich, A. Hoffmann, and B. Schuler, Proc. Natl. Acad. Sci. U. S. A. **104**, 2655 (2007).
[31] F. C. De Schryver, T. Vosch, M. Cotlet, M. Van der Auweraer, K. Mullen, and J. Hofkens, Accounts Chem. Res. **38**, 514 (2005).
[32] Multiple excitation transfer pathways are needed to describe annihilation, violating our assumption 2.